A Multi-level interface model taking into account unilateral conditions and crack evolution

Frédéric Lebon[1] Amna Rekik[2]

[1]Aix-Marseille University CNRS LMA

[2]Orléans University PRISME Institute

June 17, 2010

Outline

Bibliography

G. W. Postma, Wave propagation in a stratified medium.
Geophysics, 20, 780–806, 1955.

M. Kachanov. Solids with cracks and non-spherical pores: proper parameters of defect density and effective elastic properties.
Int. J. of Fracture, 97, 1–32 1999.

A. Rekik, F. Lebon Homogenization methods for interface modeling in damaged masonry.
Comp. and Struct., 2010.

A. Rekik, F. Lebon Identification of the representative crack length evolution in a multi-level interface model for quasi-brittle masonry.
Int. J. Sol. Struct., 2010.

Introduction

- Modeling interfaces in modern masonries
- Micro-scale effects
- Homogenization
- Asymptotic theories
- FEM implementation (CAST3M, LMGC90)

Motivations

Modeling brick masonries

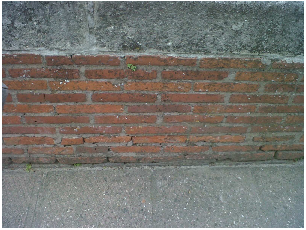

Motivations

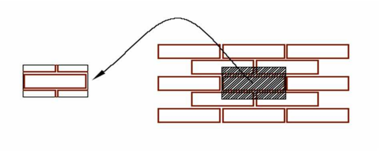

Modelling masonries at local level

- Small structures
- Assembly of bricks, mortar, interfaces (multibody mechanics)
- Mortar and bricks are deformable bodies

Hypotheses

First (Strong) Hypothesis

The brick-mortar interphase is a mixture of the two materials.

Second (Strong) Hypothesis

To simplify, the interface is a stratified.

Third Hypothesis

The interface is cracked.

Hypotheses

Fourth Hypothesis

The interface is thin.

Fifth Hypothesis

There is no penetration.

Sixth Hypothesis

The crack length increases.

Methodology: 5-step model

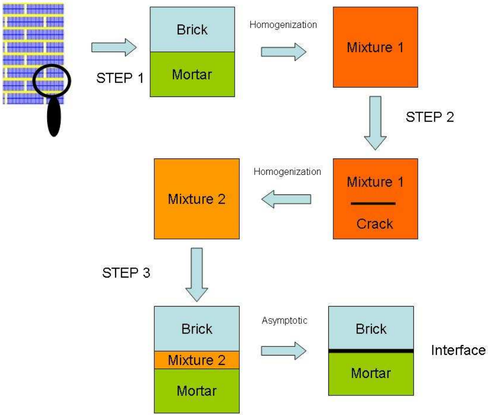

Obtain normal and tangential stiffnesses.

Step 4 Unilateral conditions Step 5 Crack evolution

First step: stratified with two phases

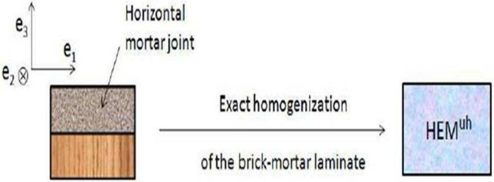

$$\begin{pmatrix} \bar{\varepsilon}_{11} \\ \bar{\varepsilon}_{22} \\ \bar{\varepsilon}_{33} \\ \sqrt{2}\bar{\varepsilon}_{23} \\ \sqrt{2}\bar{\varepsilon}_{13} \\ \sqrt{2}\bar{\varepsilon}_{12} \end{pmatrix} = \begin{pmatrix} \tilde{S}^0_{1111} & \tilde{S}^0_{1122} & \tilde{S}^0_{1133} & 0 & 0 & 0 \\ \tilde{S}^0_{1122} & \tilde{S}^0_{2222} & \tilde{S}^0_{1133} & 0 & 0 & 0 \\ \tilde{S}^0_{1133} & \tilde{S}^0_{1133} & \tilde{S}^0_{3333} & 0 & 0 & 0 \\ 0 & 0 & 0 & 2\tilde{S}^0_{1313} & 0 & 0 \\ 0 & 0 & 0 & 0 & 2\tilde{S}^0_{1313} & 0 \\ 0 & 0 & 0 & 0 & 0 & 2\tilde{S}^0_{1212} \end{pmatrix} \begin{pmatrix} \bar{\sigma}_{11} \\ \bar{\sigma}_{22} \\ \bar{\sigma}_{33} \\ \sqrt{2}\bar{\sigma}_{23} \\ \sqrt{2}\bar{\sigma}_{13} \\ \sqrt{2}\bar{\sigma}_{12} \end{pmatrix}$$

$\tilde{S}^0$ is computed exactly.

Mechanical properties of the three-fold masonry constituents

Young's moduli (MPa) of full brick	9438
Poisson ratio of full brick	0.13
Young's moduli (MPa) of hollow brick	6059
Poisson ratio of hollow brick	0.13
Young's moduli (MPa) of mortar	4000
Poisson ratio of mortar	0.3

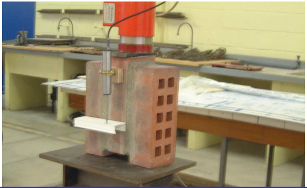

Compliance tensor

Full bricks

$$\tilde{S}^0 = 10^{-4}\begin{pmatrix} 1.478 & -0.271 & -0.348 & 0 & 0 & 0 \\ -0.271 & 1.478 & -0.348 & 0 & 0 & 0 \\ -0.348 & -0.348 & 1.639 & 0 & 0 & 0 \\ 0 & 0 & 0 & 4.444 & 0 & 0 \\ 0 & 0 & 0 & 0 & 4.444 & 0 \\ 0 & 0 & 0 & 0 & 0 & 3.499 \end{pmatrix}$$

Hollow bricks

$$\tilde{S}^0 = 10^{-4}\begin{pmatrix} 1.973 & -0.396 & -0.456 & 0 & 0 & 0 \\ -0.396 & 1.973 & -0.456 & 0 & 0 & 0 \\ -0.456 & -0.456 & 1.985 & 0 & 0 & 0 \\ 0 & 0 & 0 & 5.115 & 0 & 0 \\ 0 & 0 & 0 & 0 & 5.115 & 0 \\ 0 & 0 & 0 & 0 & 0 & 4.740 \end{pmatrix}$$

Second step: Kachanov theory

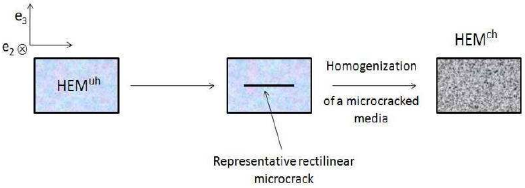

$$\frac{E_1}{E_1^0} = \frac{1}{1 + 2\rho sin^2\phi(B_{tt}cos^2\phi + B_{nn}sin^2\phi - B_{nt}sin2\phi)E_1^0}$$
$$\frac{E_3}{E_3^0} = \frac{1}{1 + 2\rho cos^2\phi(B_{tt}sin^2\phi + B_{nn}cos^2\phi + B_{nt}sin2\phi)E_3^0}$$
$$\frac{G_{13}}{G_{13}^0} = \frac{1}{1 + \rho(B_{nn}sin^2 2\phi + B_{tt}cos^2 2\phi - B_{nt}sin4\phi)G_{13}^0}$$
$$\frac{\nu_{13}}{E_1} = \frac{\nu_{13}^0}{E_1^0}$$

ϕ angle of the crack and $\rho = \sum l_k^2/A$.

Second step: Kachanov theory (continue)

$\phi = 0, \; A = eL_0$

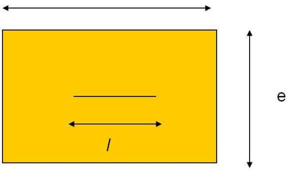

$$E_1 = E_1^0 \;\; E_3 = E_3^0/(1 + 2\rho B_{nn} E_3^0)$$
$$G_{13} = G_{13}^0/(1 + \rho B_{tt} G_{13}^0)$$
$$\nu_{13} = \nu_{13}^0$$

$B_{nn} = C(1 + D)l$ and
$B_{tt} = C(1 - D)l$

$$C = \frac{\pi}{4} \frac{\sqrt{E_1^0} + \sqrt{E_3^0}}{\sqrt{E_1^0 E_3^0}} \times \left(\frac{1}{G_{13}^0} - 2\frac{\nu_{13}^0}{E_1^0} + \frac{2}{\sqrt{E_1^0 E_3^0}} \right)^{\frac{1}{2}}$$

$$D = \frac{\sqrt{E_1^0} - \sqrt{E_3^0}}{\sqrt{E_1^0} + \sqrt{E_3^0}} \quad (1)$$

Second step: Kachanov theory (an example)

$$C_{3333} = \frac{K_1 e + K_2 l^3}{K_3 e^2 + K_4 e l^3 + K_5 l^6}$$

$$K_i(L_0, E_1, E_3, G_{13}, \nu_{13}, ...)$$

Third step: Asymptotic theory - A formal result

We introduce some notations

$$U = \{v / v \in [H^1(\Omega)]^3;\ v = 0 \ on\ \Gamma_0\}.$$

$$V = \{v \in [H^1(\Omega^+ \cup \Omega^-)]^3;\ v = 0 \ on\ \Gamma_0\}.$$

$$X = [L^2(\Omega)]^3$$

$$A^e(u, v) = \int_{\Omega_e} ae(u)e(v)\ dx + \int_{B_e} be(u)e(v)\ dx$$

$l(u) = \int_{\Omega} \varphi.u\ dx + \int_{\Gamma_1} g.u\ ds,$ with $\varphi \in [L^2(\Omega)]^3$ and $g \in [L^2(\Gamma_1)]^3$.

$$J^e(v) = \frac{1}{2}A^e(v, v) - l(v).$$

$$F^e(u) = \begin{cases} \frac{1}{2}A^e(u, u) & if\ \ u \in U \\ +\infty & if\ \ u \in X \backslash U \end{cases}$$

Third step: Asymptotic theory - A formal result

Theorem

Under the previous assumptions, F^e Γ-converges to F^0 at point u with

$$F^0(u) = \begin{cases} \frac{1}{2}\int_\Omega ae(u)e(v)\ dx + \frac{1}{2}\int_S \bar{b}([u]\otimes_s n)([u]\otimes_s n)\ ds \\ if\ \ u \in V \\ +\infty\ \ if\ \ not \end{cases}$$

The term $[u]$ is the jump of displacement along the interface S.
We can observe that the jump along the interface S is given by:

$$\sigma n = \bar{b}([u]\otimes_s n)n,\ \ \bar{b} = \lim\ \ b/e$$

Proof: generalization of a result by Licht-Michaille, 1996.

Third step: Asymptotic theory

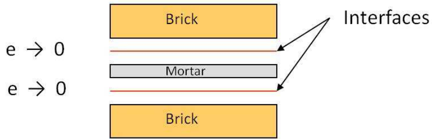

$$\sigma n = C(l, ...)[u]$$

$$C_{3333} \rightarrow C_N = \frac{L_0}{2C(1+D)\, l^3} \quad C_{1313} \rightarrow C_T = \frac{L_0}{4C(1-D)\, l^3}$$

Third step: Asymptotic theory

Full Bricks
$C_N = 242365/l^3 \, (N/mm^2)$ and $C_T = 127600/l^3 \, (N/mm^2)$

Hollow Bricks
$C_N = 200396/l^3 \, (N/mm^2)$ and $C_T = 100490/l^3 \, (N/mm^2)$

Fourth step: Unilateral contact

Let F be the density of the contact forces.

$$F = F_n n^b + F_t, \quad \text{with} \quad F_n = F.n^b$$

Locally, the unilateral contact is given by the following relations

$$[u_n] \geq 0, \quad F_n - C_N[u_n] \geq 0, \quad \text{and} \quad (F_n - C_N[u_n])[u_n] = 0$$

Fifth step: Crack evolution

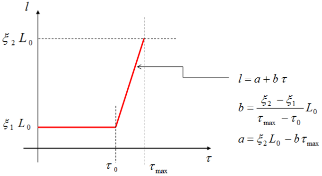

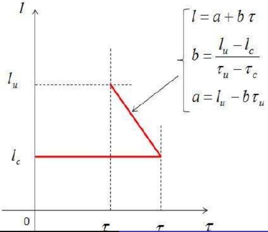

Numerical results

- Without confinement (Fouchal)
- With confinement (Gabor)
- RILEM test (diagonal compression)

Numerical results: triplet of full bricks

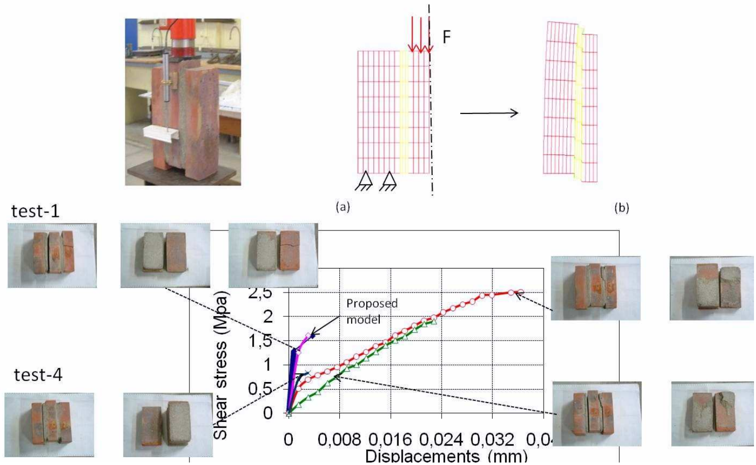

Numerical results: triplet of full bricks

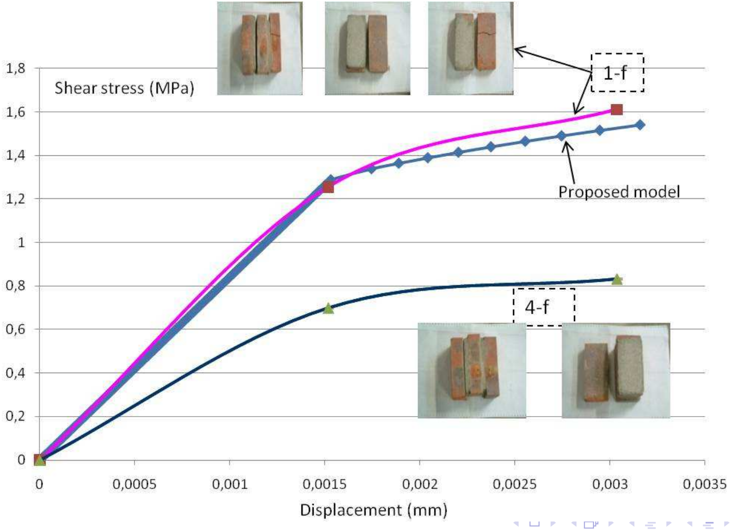

Numerical results: triplet of hollow bricks

test-1

test-2

test-3

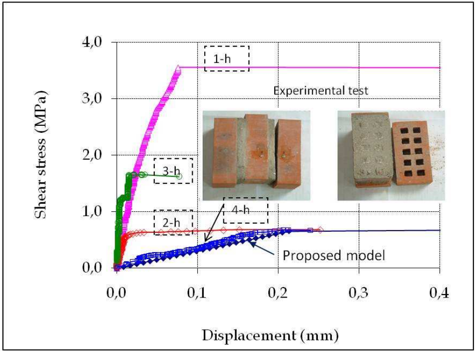

Numerical results: Identification

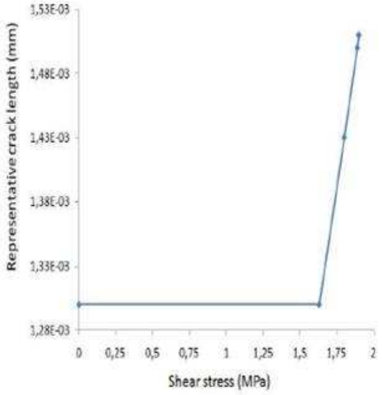

Numerical results: confined small prism

Various confinement pressures

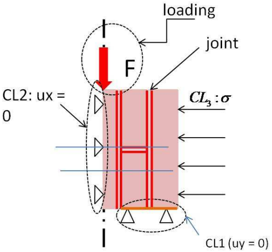

Brick: 210x50x100 mm3, Eb = 12800 MPa, $\nu_b = 0{,}2$
Mortar: thickness 10 mm, Em = 4000 Mpa, $\nu_m = 0{,}2$
Joints: CN and CT

$\sigma = 0, 0{,}2, 0{,}4, \ldots, 1{,}6 MPa$

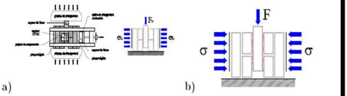

FIG. 4.8 – Dispositif d'essai de cisaillement pour prismes de maçonnerie

x

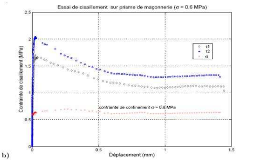

FIG. 4.10 – a) Courbe $\tau - \delta$ pour $\sigma = 0,4\ MPa$. b) Courbe $\tau - \delta$ pour $\sigma = 0,6\ MPa$.

Softening effect

Numerical results: confined small prism

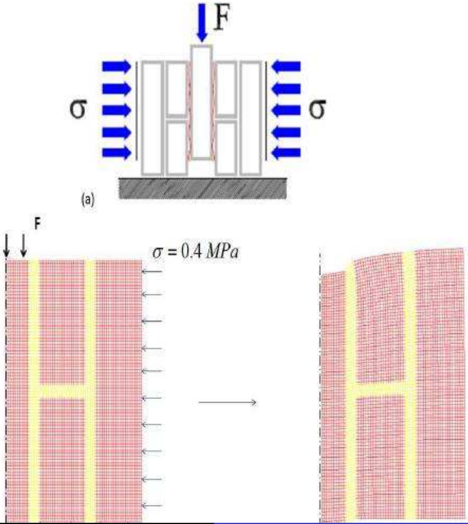

Numerical results: confined small prism

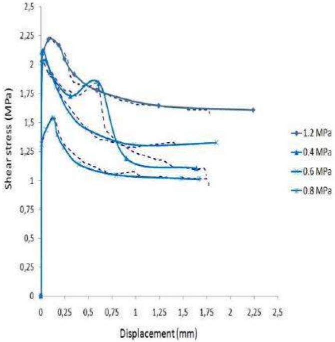

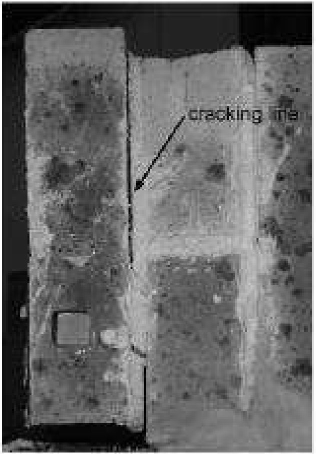

Numerical results: Identification

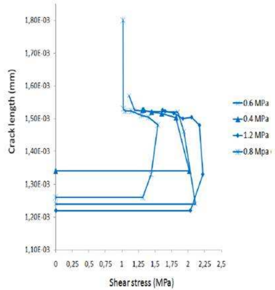

confining stress σ (MPa)	l_u (μm)	$e_r(l_u)$ (%)
0.4	1.57	2.5
0.6	1.53	5
0.8	1.8	11.1
1.2	1.53	5

Numerical results: Rilem test

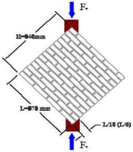

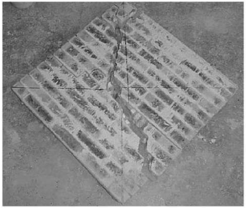

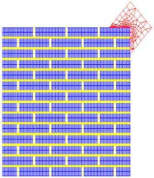

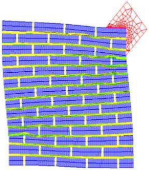

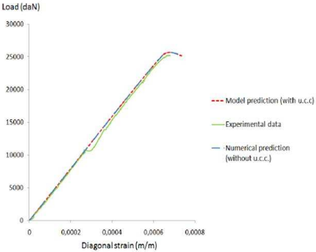

Unilateral contact

unilateral contact condition	l_u (μm)	$e_r(l_u)$ (%)
with	1.61	3
without	1.728	4

Table: Identified ultimate representative crack length and the corresponding relative errors obtained on a diagonally compressed wall with and without a unilateral contact condition

Conclusion

- Model of interface taking into account fissuration evolution
- Implementation (Cast3M)
- Comparison with experimental data and identification

Five improvements

- Dynamics (collaboration F. Dubois, Montpellier)
- 3D (coupling in-plane and out-of-plane)
- Improve Kachanov model
- Coupling surface and volume damage
- Evolution of fissure length

Thank you for your attention !